A novel role of AURKA kinase in erythroblast enucleation

Yuanlin Xu,[1,2*] Peijun Jia,[1*] Yating Li,[1*] Huan Zhang,1 Jingxin Zhang,[1] Wanxin Li,[1] Yazhe Zhen,[1] Yan Li,[1] Jiaming Cao,[1] Tingting Zheng,[1] Yihan Wang,[2] Yanyan Liu,[2] Xiuli An[3#] and Shijie Zhang[1#]

[1]School of Life Sciences, Zhengzhou University, Zhengzhou, China; [2]Department of Internal Medicine, The Affiliated Cancer Hospital of Zhengzhou University & Henan Cancer Hospital, Zhengzhou, China and [3]Laboratory of Membrane Biology, New York Blood Center, New York, NY, USA

[*]YX, PJ and YL contributed equally as first authors.
[#]XA and SZ contributed equally as senior authors.

Correspondence: S. Zhang
shijie-zhang@zzu.edu.cn

X. An
xan@nybc.org

Received: December 16, 2023.
Accepted: June 7, 2024.
Early view: July 4, 2024.

https://doi.org/10.3324/haematol.2023.284873

Supplementary methods

Ubiquitylation assay. Cells were transfected with plasmids expressing Myc-Ub for 48 h, with or without His-AURKA and/or GST-ECT2 vectors. Cells were collected and washed in cold PBS after treated with MG132 (Sigma-Aldrich) for 6 h and then lysed in RIPA lysis buffer (Cowin Biotechnology) containing phosphatase inhibitors and protease inhibitor. Cell lysates were incubated with magnetic protein A/G beads (Bio-Rad) for 2 hours, followed by immunoprecipitation using anti-AURKA antibody for 12 hours at 4°C and subsequent washing. The immunoprecipitation mixture was boiled in the SDS sample buffer, separated by 10% SDS-PAGE, transferred onto a nitrocellulose membrane (Bio-Rad), and subjected to Western blotting procedures.

Overexpression of ECT2 in $CD34^+$ Cells. The ECT2 gene was cloned into the pLVX-puro lentiviral vector. The ECT2 coding sequence was inserted into the pLVX-puro vector backbone through standard molecular cloning techniques, and the integrity of the construct was confirmed by DNA sequencing. Human $CD34^+$ hematopoietic stem cells were transduced with the recombinant pLVX-puro-ECT2 lentivirus. Following transduction, the cells were selected with puromycin for 3 days to enrich for populations expressing ECT2. The overexpression of ECT2 was confirmed by quantitative PCR to ensure efficient transduction and expression within the cells.

Imaging flow cytometry. Terminal erythroid cells differentiated from $CD34^+$ cells were fixed and then stained with antibodies specific for AURKA and ECT2. After staining, the cells were analyzed using an Image Stream X Mark II (ISX-100, Amnis/Luminex), and the images were subsequently analyzed using the IDEAS software (Amnis).

Supplementary Figure Legends

Supplemental Figure 1. Efficient AURKA knockdown impacts erythroblast enucleation and nuclear polarization.

(A) Schematic diagram of enucleation in human $CD34^+$ cells followed by erythroid cell culture. (B) Flow cytometry gating strategy was utilized for enucleation of sorted mouse bone marrow orthochromatic erythroblasts, followed by an 18 hours culture period. (C) Enucleation was assessed in the presence or absence of MLN8237 for sorted mouse orthochromatic erythroblasts for 18 hours. (D) Model of a

siRNA-mediated knockdown approach in human erythroblasts. (E) Effective downregulation of AURKA in human erythroblasts confirmed by western blot analysis following treatment with three distinct AURKA siRNA oligonucleotides and scramble siRNA. (F) Quantitative analysis showing nuclear and cellular dimensions in MLN8237-treated and control erythroblasts. (G) Representative cytospin images displaying the extent of enucleation in erythroblasts treated with AURKA-specific siRNA and control. Scale bar = 10 μm. (H) Quantitative assessment of the mean Δ centroid in erythroblasts treated with AURKA-specific siRNA and control.

Supplemental Figure 2. Dynamic changes in AURKA localization during erythroblast enucleation in mice.

Confocal microscopy images capturing AURKA distribution (red) through different stages of erythroblast enucleation in mouse cells. Ter119 antibody, marking the erythroid cell membrane, and Hoechst33342, staining the nucleus, are used to delineate cellular components. Scale bar=5 μm.

Supplemental Figure 3. Effect of AURKA-specific siRNAs on the location of AURKA and γ-tubulin during erythroblast enucleation.

(A) Co-immunoprecipitation (co-IP) showed a direct interaction between AURKA and γ-tubulin. (B) Representative Western blots showed the protein levels of γ-tubulin in hemin-treated or untreated K562 cells cultured with indicated concentrations of MLN8237. (C) Quantitative analysis showed γ-tubulin protein levels. Confocal microscope images showed the colocalization of AURKA and γ-tubulin in non-polarized cells (D), polarized cells (E) and enucleating cells (F) treated with AURKA-specific siRNA. Scale bar=5 μm.

Supplemental Figure 4. Dynamic interaction between AURKA and ECT2 during erythroblast enucleation, observed through Image Stream analysis.

This series of high-resolution images captures the evolving relationship between AURKA and ECT2 in polarization (A) and enucleting (B) stages of erythroblast through image stream analysis. Scale bar=7 μm. (C) Quantitative analysis of the distance of AURKA foci to the center of cytoplasm. (D) Quantitative analysis of the distance of the center of ECT2 fluorescence to the center of nucleus.

Supplemental Figure 5. Impact of AURKA inhibition on ECT2 translocation in mice bone marrow erythroblasts.

Confocal microscope images showed cellular localization of ECT2 in non-polarized cells (A), polarized cells (B) and enucleating cells (C) after treatment with or without MLN8237 in mice bone marrow erythroblasts. Scale bar=5 μm.

Supplemental Figure 6. Effects of ECT2 over-expression on erythroblast differentiation and enucleation.

(A) PCR analysis confirming significant up-regulation of ECT2 expression in $CD34^+$ cells following transfection with ECT2 over-expression vectors, establishing effective gene manipulation. (B-C) Analysis of erythroid differentiation in cells over-expressing ECT2, showing minimal changes compared to control groups. (D-F) Quantitative and qualitative assessments of enucleation in erythroblasts with elevated ECT2 levels.

Supplemental Figure 7. ECT2 knockdown mitigates enucleation deficits in AURKA-inhibited erythroblasts.

(A) PCR analysis confirmed significant downregulation of ECT2 expression after treatment with three distinct siRNA oligonucleotides. (B) Examination of erythroblast enucleation following transfection with ECT2-specific siRNA and control. (C-D) Representative cytospin images displaying erythroblast enucleation in cells co-treated with MLN8237 (10 μM or 100 μM) and ECT2-specific siRNA. Scale bar = 10 μm.

Figure S1

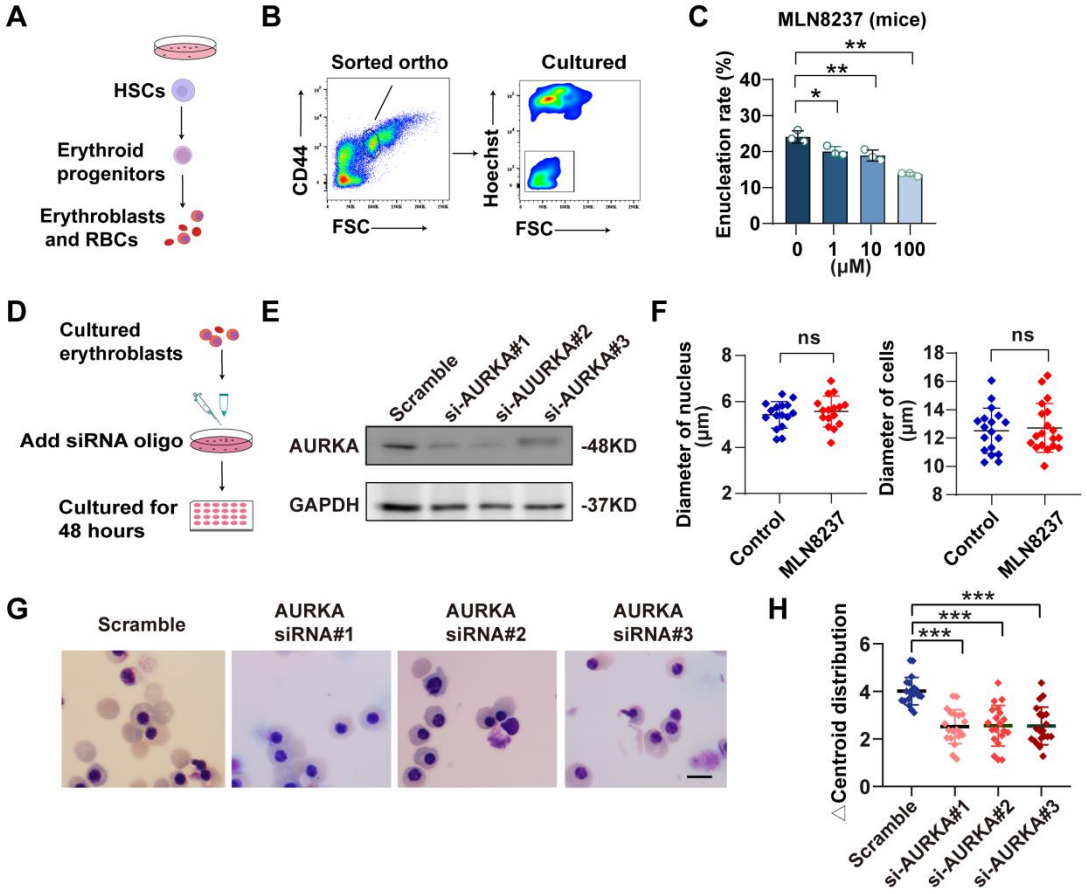

Supplemental Figure 1. Efficient AURKA knockdown impacts erythroblast enucleation and nuclear polarization.

Figure S2

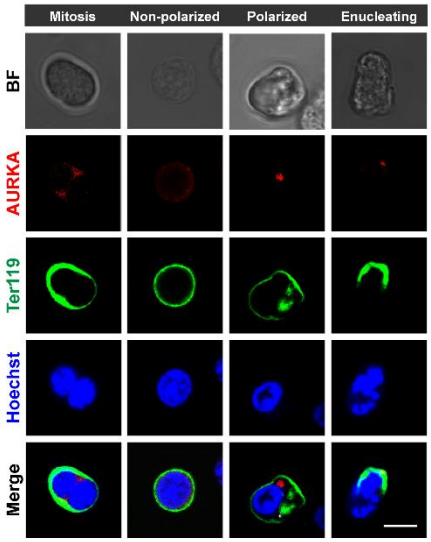

Supplemental Figure 2. Dynamic changes in AURKA localization during

erythroblast enucleation in mice.

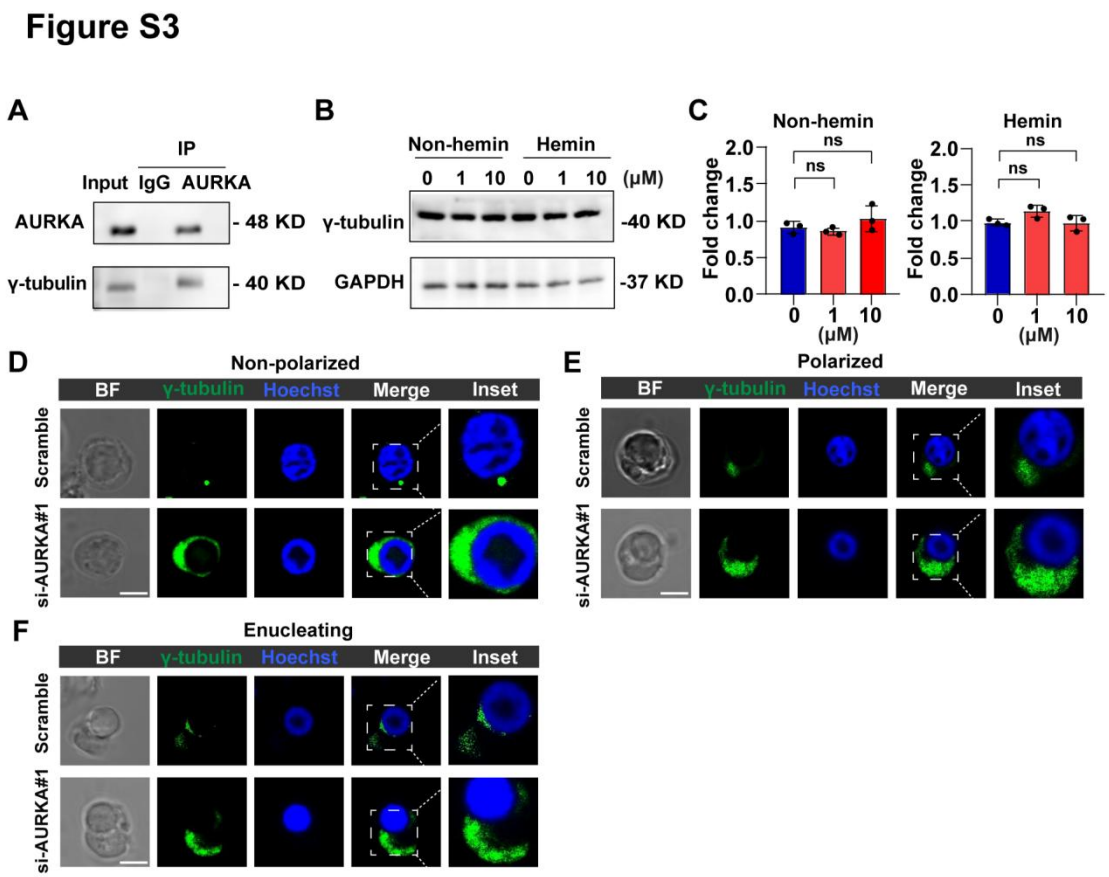

Supplemental Figure 3. Effect of AURKA-specific siRNAs on the location of γ-tubulin during erythroblast enucleation.

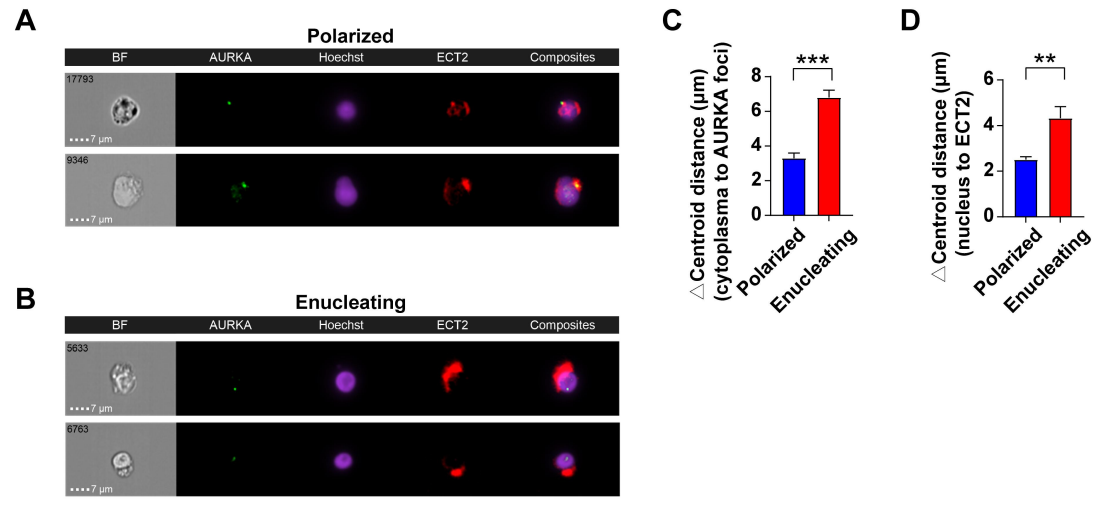

Supplemental Figure 4. Dynamic interaction between AURKA and ECT2 during

erythroblast enucleation, observed through Image Stream analysis.

Figure S5

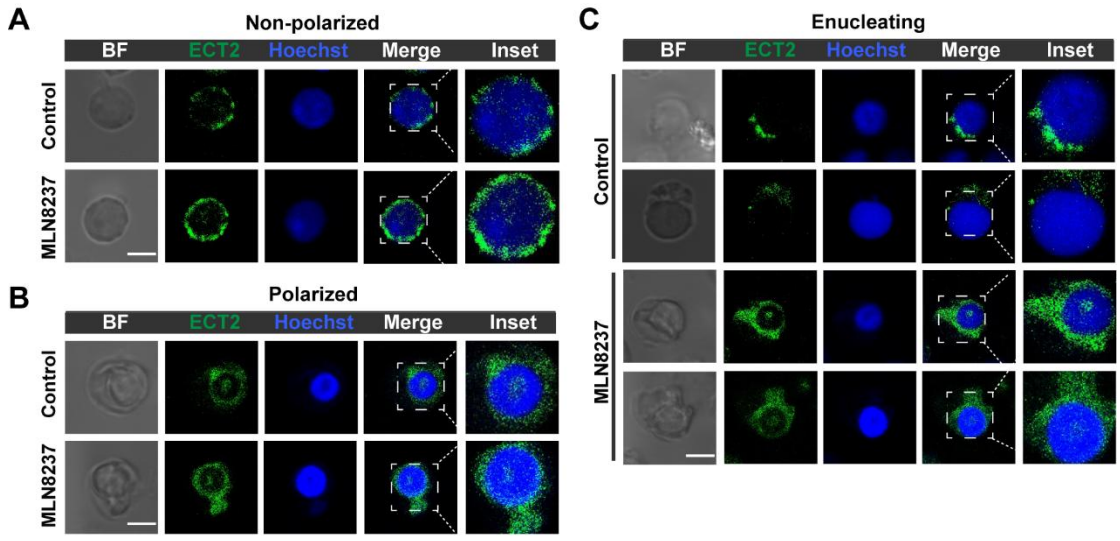

Supplemental Figure 5. Impact of AURKA inhibition on ECT2 translocation in mice bone marrow erythroblasts.

Figure S6

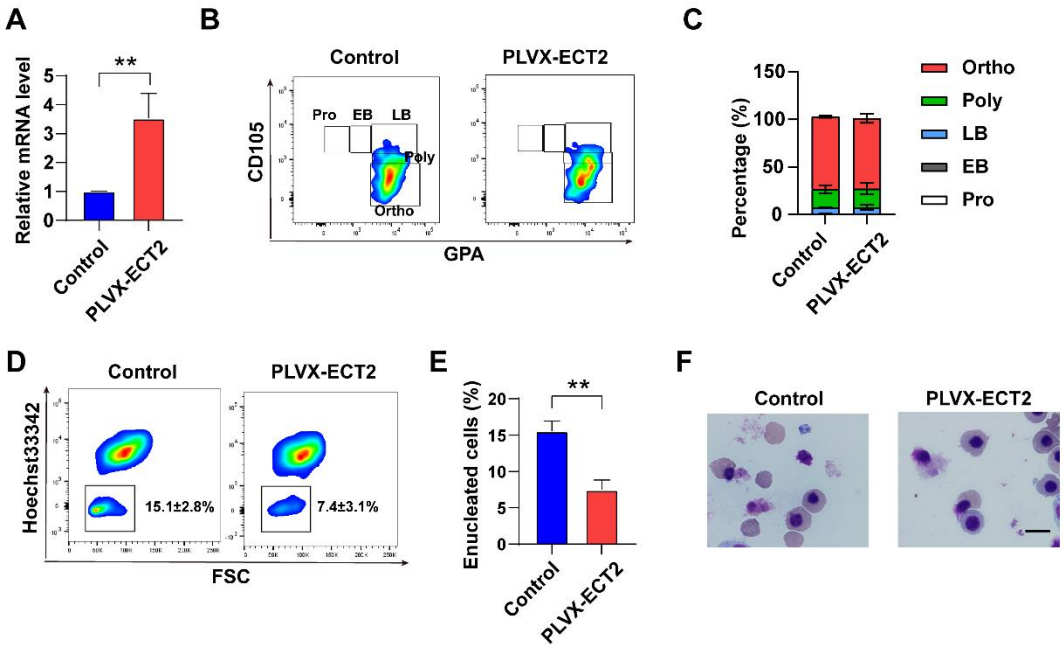

Supplemental Figure 6. Effects of ECT2 overexpression on erythroblast differentiation and enucleation.

Figure S7

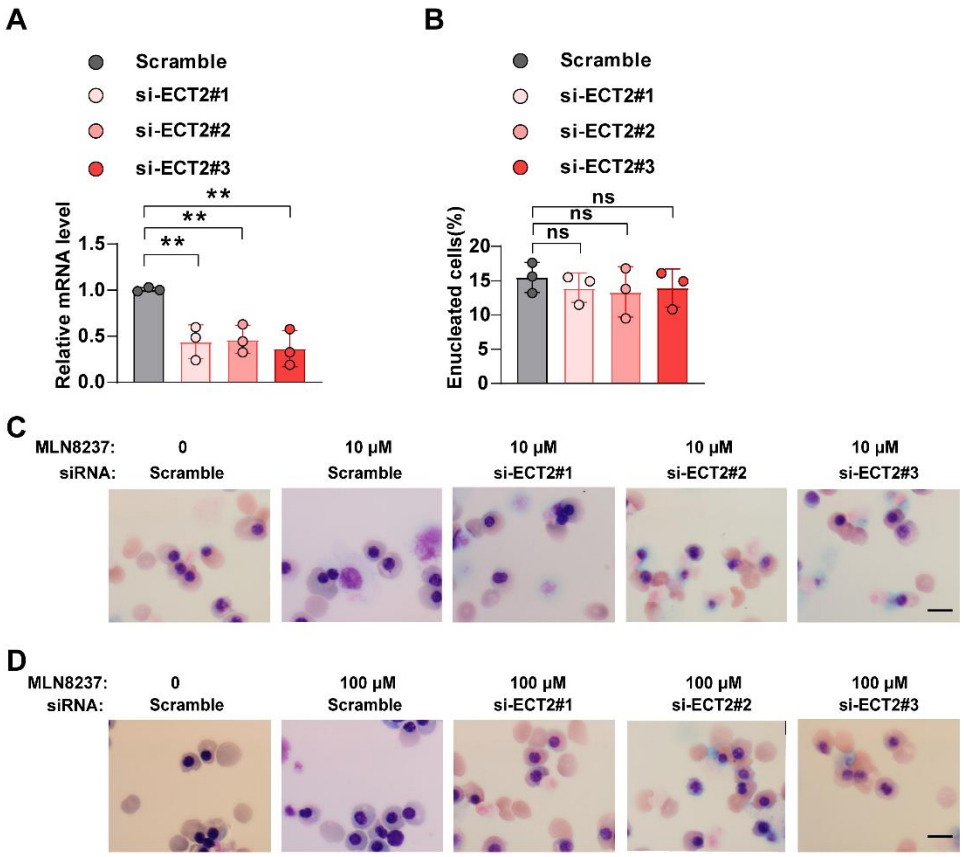

Supplemental Figure 7. ECT2 knockdown mitigates enucleation deficits in AURKA-inhibited erythroblasts.

Supplemental Table 1. Antibodies for Western blotting and immunofluorescence

Antibodies	Antibodies	working concentration	company
AURKA	Rabbit monoclonal antibody	1：1000	Cell Signaling Technology
AURKB	Rabbit monoclonal antibody	1：1000	Cell Signaling Technology
Anti-gamma Tubulin	Rabbit monoclonal antibody	1：1000	Abcam
ECT2	Murine monoclonal antibody	1：1000	Santa Cruz Biotechnology
GAPDH	Murine monoclonal antibody	1：1000	Proteintech
Goat Anti Rabbit	-	1：2000	Proteintech
Goat Anti Mouse	-	1：2000	Proteintech
AURKB	Rabbit monoclonal antibody	1：100	Cell Signaling Technology
AURKB	Rabbit monoclonal antibody	1：100	Cell Signaling Technology
AURKA	Rabbit monoclonal antibody	1：100	Signalway Antibody
ECT2	Murine monoclonal antibody	1：100	Santa Cruz Biotechnology
Hochest33342	-	1：100	Solarbio
Mouse Anti-γ Tubulin antibody	Murine monoclonal antibody	1：100	Bioss
Actin-Tracker Green	-	1：100	Beyotine
Goat Anti Mice FITC	-	1：100	Solarbio
Goat Anti Rabbit RBITC	-	1：100	Bioss

Supplemental Table 2. qRT-PCR primers

Gene	Primer
AURKA：	Forward：GAGGTCCAAAACGTGTTCTCG
	Reverse：ACAGGATGAGGTACACTGGTTG
AURKB：	Forward：CAGTGGGACACCCGACATC
	Reverse：GTACACGTTTCCAAACTTGCC
TUBG1：	Forward：AGCTGGTGTCTACCATCATGT
	Reverse：CGTAGTGAGAGGGGTGTAGC
ECT2：	Forward：ACTACTGGGAGGACTAGCTTG
	Reverse：CACTCTTGTTTCAATCTGAGGCA

Supplemental Table 3. The siRNA sequences and overexpression primers

Primer name：	Primer sequence：
ECT2-siRNA (#1)	forward primer：GCGGGUUGAAACAAUUUCUTT
	Reverse primer：AGAAAUUGUUUCAACCCGCTT
ECT2-siRNA (#2)	forward primer：GACCACCAGUUGUAUUAAATT
	Reverse primer：UUUAAUACAACUGGUGGUCTT
ECT2-siRNA (#3)	forward primer：GAAGCCAGAAUGGAUUUAUTT
	Reverse primer：AUAAAUCCAUUCUGGCUUCTT
AURKA-siRNA (#1)	forward primer：GCCGGUUCAGAAUCAGAAGTT
	Reverse primer：CUUCUGAUUCUGAACCGGCTT
AURKA-siRNA (#2)	forward primer：GGCUCUUAAAGUGUUAUUUTT
	Reverse primer：AAAUAACACUUUAAGAGCCTT
AURKA-siRNA (#3)	forward primer：GCAAUUUCCUUGUCAGAAUTT
	Reverse primer：AUUCUGACAAGGAAAUUGCTT
ECT2-overexpress -plvx	forward primer：GGATCTTCCAGAGATGGATCCATGGCTGAAAATA GTGTATTAACATCC
	Reverse primer：CTGCCGTTCGACGATCTCGAGTCATATCAAATGA GTTGTAGATCTACTTAACG